https://doi.org/10.3311/PPci.38197

Periodica Polytechnica Civil Engineering, 69(2), pp. 363–372, 2025

Evaluation of Dynamic Properties of Sand Mixed with Expanded Glass Granules by Energy Concept Under Cyclic Torsional Loadings

Seyfettin Umut Umu[1*]

[1] Vocational School of Transportation, Eskisehir Technical University (ESTU), Basin Sehitleri 152., 26140 Eskisehir, Türkiye
[*] Corresponding author, e-mail: suumu@eskisehir.edu.tr

Received: 27 August 2024, Accepted: 01 December 2024, Published online: 06 December 2024

Abstract

In recent years, lightweight materials have gained attention for their numerous benefits, including cost reduction, insulation, and bearing capacity. Expanded glass granules (EGG) stand out among these materials, showing significant potential in geotechnical engineering applications. This study examines the potential use and feasibility of a SAND-EGG mixture in geotechnical applications through cyclic torsional shear test for measuring shear strength, modulus reduction, and energy dissipation. This is conducted on the unmixed dry specimens (Reference Sand, EGG) and the mixed dry specimens by mass (1, 2%) and volume (5, 10, 15%) under 100 kPa effective pressure. The test also conducted along 0.02%–0.5% shear strain amplitudes for both samples group. An energy-based approach is used to analyze mixed material's capacity for energy dissipation, a crucial factor in determining seismic resistance during cyclic loading. The impact of employing EGG on modulus reduction behavior was also explored concerning energy dissipation. Considering the results, it is show that the use of EGG increases the resilience with high friction capacity and by taking up a significant portion of the available void ratio and provides lightness in geotechnical applications in examined shear strain amplitude range (0.02%–0.5%).

Keywords

sand, expanded glass granules, dynamic torsional test, energy dissipation, shear strength, modulus reduction

1 Introduction

The planet's escalating waste crisis is further compounded by limited storage capacities, which impede effective management. The recycling of these by-products for engineering purposes represents a viable solution [1, 2]. Projected to double by 2050 and triple by 2100 [3], global waste output includes around 30% from construction, responsible for over one-third of global carbon emissions. Consequently, efficient waste management is critical to limit landfill reliance. Utilizing construction waste in geotechnical projects could substantially reduce energy demands for natural aggregate extraction and landfill processing [4, 5]. Moreover, by recycling glass, it is possible to replace 1.2 times its weight in virgin materials, leading to lower CO_2 emissions and decreased reliance on natural resources [6].

In geotechnical engineering, soil has been stabilized mainly with lime, calcareous additives, bitumen, and cement [7–10]. New findings, however, highlight that materials like fly ash, geosynthetics, crumb rubber, polymers, EPS, marble and stone waste, and glass may perform similarly [11–13]. Furthermore, comprehensive shake table tests have assessed the liquefaction resistance of sand-tire chip composites [14–16].

This research examines the cyclic load behavior of expanded glass granules (EGG), derived from recycled glass (RG) and used with sand as an additive. EGG production involves waste glass crushing, contaminant removal (such as aluminum and steel), and fine grinding, which is critical to foam glass quality. Before expansion, a foaming agent and binder are added. Integrating EGG into production enhances building and industrial materials, promoting high-quality structural and specialized products [6, 17, 18]. When blended with blowing agents and melted at elevated temperatures, RG becomes granules of various sizes (0.045–16 mm), with bulk densities ranging from 140 to 500 kg/m^3. The porous EGG structure provides notable insulation and acoustic efficiency by trapping air in its pores [19, 20].

Cite this article as: Umu, S. U. "Evaluation of Dynamic Properties of Sand Mixed with Expanded Glass Granules by Energy Concept Under Cyclic Torsional Loadings", Periodica Polytechnica Civil Engineering, 69(2), pp. 363–372, 2025. https://doi.org/10.3311/PPci.38197

In geotechnical fields like infrastructure, slope stabilization etc., the adoption of recycled materials, particularly glass, has become increasingly popular due to their strong endurance and ecological benefits. According to Disfani et al. [1], fine and medium glass display shear strength close to natural sand (RS) and gravel with angular particles, meeting fill material standards [1, 21–23]. Recent studies indicate that RG, which shares properties with RS, is an effective alternative material in both superstructure and infrastructure geotechnical projects. Experimental study conducted by Umu [24], the combination of EGG and kaolinite clay was investigated and the results demonstrated that glass granules can be employed for shallow soil stabilization due to their high internal friction angle [24–26]. The experimental study by Yaghoubi et al. [27] evaluated the impact of adding RG to high-plasticity expansive clay as a non-chemical soil treatment. Clay was mixed with RG, and the resilient modulus properties were measured and incorporated into finite element models of pavement systems. The results revealed that adding RG significantly increased the resilient modulus and reduced strains under load [27]. Moreover, empirical evidence indicates that the particle size and shape (angular or rounded) of glass impact its geotechnical performance, highlighting its sustainable and viable use in eco-friendly construction [28].

Seismic risk assessment focuses on understanding structural responses to seismic events, such as earthquakes and blasts, with dynamic behavior of soil as a key factor during seismic wave movement. A comprehensive grasp of these soil behaviors is crucial for predicting damage and engineering resilient solutions. Seismically hazardous soil resistance is often evaluated using stress- and strain-based methods [29, 30]. An alternative approach considers energy dissipation in soil layers as seismic waves move through, instead of focusing solely on cyclic shear stress or strain [31–33]. The method assumes cyclic deformation dissipates energy in the soil, with part absorbed by the soil matrix, and quantifies the dissipated energy per unit volume through the hysteresis loop area. Research shows the energy-based method may be superior for identifying seismically risky soils, correlating with dynamic strength and residual strain [34–36].

The aim of this study is to investigate the dynamic behavior of RS mixed with EGG by means of dynamic torsional shear tests using an energy-based approach. The dry mixtures, prepared by mass (1, 2%) and by volume (5, 10, 15%), were subjected to cyclic loading with shear strain amplitudes varying from 0.02% to 0.5% at 100 kPa. To fully understand the effect of EGG on RS, the tests were conducted in a manner that excluded the dynamic influences of water. The results strongly support that EGG increases shear modulus and modulus reduction through energy dissipation under cyclic loading highlighting its potential to enhance shallow soil stabilization.

2 Test method and basic considerations

Previous research has established a direct relationship between energy dissipation and dynamic soil responses, focusing on dynamic strength, shear modulus and permanent strain. The dissipation energy is quantified by assessing energy losses during deformation cycles, usually by direct specimen measurement. In two-dimensional stress space, energy loss is represented by the area of the hysteresis loop. This enclosed area in the stress-strain curve defines the total energy dissipated per unit volume (ΔW), calculated using Eq. (1) for torsional shear [31, 37, 38].

$$\Delta W = \sum_{i=1}^{n-1} 0.5\left(\tau_{i+1} + \tau_i\right)\left(\gamma_{i+1} - \gamma_i\right) \tag{1}$$

In a loading history, n refers to the number of recorded points, γ is the shear strain amplitude, τ denotes shear stress, and ΔW indicates energy loss per unit volume. The determination of critical energy is feasible in conventional cyclic laboratory tests, like dynamic torsional shear, provided that data acquisition is fast and hysteretic loops are closely spaced. The key benefits of the energy approach compared to other techniques include [39, 40]:

1. The intensity of dynamic loading exhibits a direct correlation with energy.
2. Analyzing the historical shear stress and determining the corresponding number of uniform cycles at specific stress or strain levels is unnecessary.
3. In all cases, a simple sinusoidal loading pattern can be utilized due to its practical independence from the load waveform. This eliminates the necessity to simulate intricate random stress histories during laboratory experiments.
4. In every scenario, a basic sinusoidal loading pattern suffices, as it is essentially unaffected by the load waveform and obviates the requirement to simulate complex random stress histories in laboratory experiments.

The dissipated energy consists of two primary components: the first arises from particle rearrangement and bond distortion, leading to plastic strain, while the second involves energy accumulation as heat, kinetic or surface energy, increasing the mobility of soil particles. This accumulation during successive cycles contributes significantly to the dynamic instability of soils [38].

The study employed a dynamic torsional shear device, powered by an AC servo motor, in the geotechnical laboratory at Eskisehir Osmangazi University (Fig. 1). The Resonant Column/Torsional Shear Test System (RCTS) reliably measures dynamic soil properties based on wave propagation theory in prismatic rods, making it a key experimental tool in soil dynamics assessment. The RCTS is capable of measuring along shear strain amplitude γ = 0.0001%–1% and this allows the test system to be used to measure dynamic soil parameters in the relevant range. Different deformation measurement apparatus can be added to the test system to extend shear strain amplitude spectrum [41]. In the laboratory experiments, cyclic torsional stress was applied under undrained conditions, beginning with low shear strain amplitudes. The shear strain amplitudes were systematically increased to span a shear strain amplitude range of 0.02% to 0.5%, all while keeping the confining pressure constant at 100 kPa.

Fig. 1 Torsional shear test device

3 Materials, preparation and loading parameters

The RS, containing 98% silica, is a non-uniform sand and a grain diameter that is, in general, approximately spherical (Table 1).

After the completion of the production process, the EGG are subjected to a sieving procedure that yields a specific gradation. Prior to the selection of the specific EGG size for the current research endeavor, comprehensive resonant column tests were executed (Fig. 1), encompassed a graduation from 0.25 to 8 mm. Results showed that EGG with 2–4 mm diameters exhibited a higher shear modulus than other sizes.

The granular structure of EGG enables the retention of heat through the trapping of air within its matrix. Its hollow design limits water absorption to 15% of overall weight, even if it's entirely flooded, thereby ensuring long-term thermal insulation and stability. Additionally, EGG exhibits resistance to a wide range of chemical agents and does not degrade, enhancing its applicability. This durability can be attributed to the enclosed cavities within the EGG pores, which preserve its properties and structural integrity over time [20]. Laboratory properties from the EGG manufacturer are shown in Table 2. The testing involved dry mixed samples with volume ratios of 5%, 10%, and 15%, and mass ratios of 1% and 2%. The RS and EGG were mechanically mixed in a pan for a specific duration to ensure uniformity, considering the specified proportions (Fig. 2). Recognizing the critical role of water in granular soil behavior under cyclic dynamic loading, samples were prepared in a fully dry state to assess the dynamic interplay of granules with sand particles. The samples were then positioned in the dynamic torsional shear test apparatus according to the specifications outlined in Table 3. Grain size distribution of the RS and EGG given in Fig. 3. Angle of internal friction values of mixed sample, determined at laboratory, given in Fig. 4.

In the cyclic dynamic torsional shear test, torque is applied to specimens at a specific frequency, regulating shear strain amplitude until collapse or the measurement

Table 1 The laboratory characteristics of RS

	$D_{10,50}$ (mm)	U_C	C_C	ϕ	G_s	$e_{min,max}$
RS	0.63–0.13	6	1.28	33º	2.637	0.674–0.415

$D_{10,50}$: Effective and mean grain diameter; U_C, C_C: Cofficient of uniformity and curvature; G_s: Specific gravity; ϕ: Angle of internal friction; $e_{min,max}$: Minimum, maximum void ratio

Table 2 Laboratory properties of EGG

	G_s	φ	WA%	D (mm)	$\rho_{d(max)}$ (gr/cm^3)	CS (MPa)	CaO + MgO	SiO_2	Al_2O_3	$Ka_2O + Na_2O$	pH	Fe_2O_3	HR/Melt (°C)
EGG	0.34	45°	15	2–4	0.276	1.4	8/10.5	71/73	1.5/2.0	13/14	9/11	<0.3	750/1000

G_s: Relative density (Mg/m^3); φ: Angle of internal friction; D: Used size of EGG; CS: Compressive strength; WA: Water absorption by mass; HR: Heat resistant

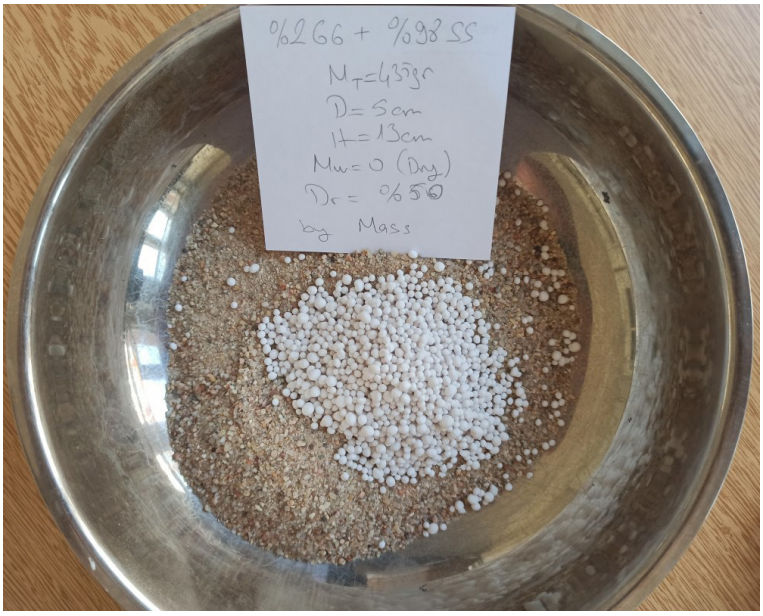

Fig. 2 The exemplary mixture sample which contains (2EGG98RS)

Table 3 Test specifications of mixed (by volume and by mass) and reference samples

		Non-mixed		Mixed by volume			Mixed by mass	
		100EGG	100RS	95RS5EGG	90RS10EGG	85RS15EGG	99RS1EGG	98RS2EGG
	EGG	70.19	0	3.51	7.05	10.53	4.35	8.70
M_T (g)	RS	0	435	413.48	391.72	369.96	430.65	426.30
	Total	70.19	435	416.99	398.74	380.49	435	435
M_W (g)					0			
V_T (cm^3)					255.25			
R (mm)					50			
H (mm)					130			
ρ_d (gr/cm^3)		0.276	1.704	1.633	1.562	1.49	1.704	1.704

M_T and M_W: Total and water mass; V_T: Total volume; ρ_d: Dry density; R and H: Sample diameter and height

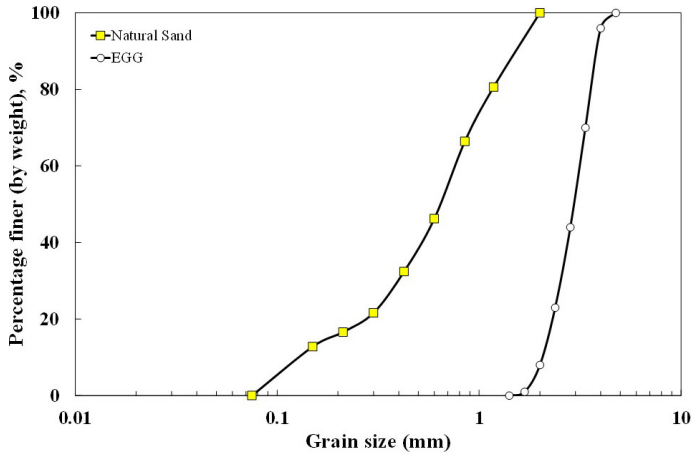

Fig. 3 Grain size distribution of RS and EGG

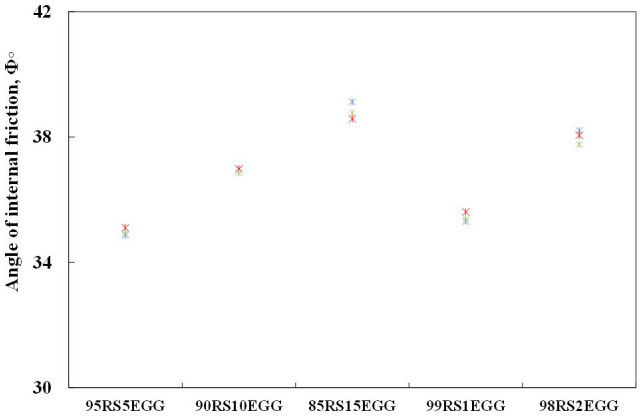

Fig. 4 Angle of internal friction values of mixed samples

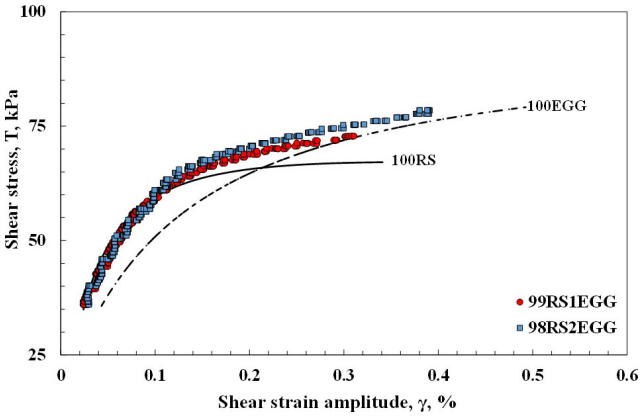

Fig. 6 Stress and strain variation of 99RS1EGG and 98RS2EGG

limit is reached. Recorded data includes torque level, cycle count, shear deformation amplitude, shear stress, and shear modulus. The initial torque was set at 40 pfs, increasing by 1 pfs every 10 cycles. Loading parameters applied on all samples are presented in Table 4.

4 Experimental results

4.1 Shear stress and shear strain results

Experiments were performed on reference sand (100RS) and EGG (100EGG). The cyclic dynamic torsional shear test results in Fig. 5 reveal that RS100 demonstrates linear elastic behavior at shear strain amplitudes of 0.02% to 0.1%, before shifting to non-linear behavior. Conversely, the 100EGG curve does not exhibit a clear linear region and shows a steady increase in stress with shear strain, due to the nearly spherical shape of EGG particles and their high internal friction angle. Fig. 6 presents the stress-shear strain graphs for the 99RS1EGG and 98RS2EGG specimens, which have the same dry unit density as 100RS (Table 3). Initially, both mixtures behave like 100RS within the shear strain range of 0.02% to 0.1%. However, as shear strain increases, the behavior is markedly influenced by EGG, due to its high internal friction angle and ability to fill voids.

The stress-shear strain deformation graphs of 95RS5EGG, 90RS10EGG and 85RS15EGG mixed specimens prepared by volume in Fig. 7.

The dry unit densities of all three samples are approximately 5%, 9% and 14% lower than the RS, respectively. Within a shear strain range of 0.02% to 0.2%, the 95RS5EGG sample behaves similarly to 100RS, with EGG's influence increasing beyond this range. The 90RS10EGG sample, while comparable to 100RS, presents lower values (Fig. 5). The 85RS15EGG specimen, dominated by EGG at all shear strain levels, exhibits greater strength than EGG but less than RS due to a lower dry unit density (Fig. 7).

Table 4 Loading parameters acting on the specimens

Initial torque (pfs)	Torque increment (pfs)/Cycle	Loading frequency (Hz)
40	1/10	1

pfs = Max. Torque is 200 pfs. 200 pfs = 2.5 N m

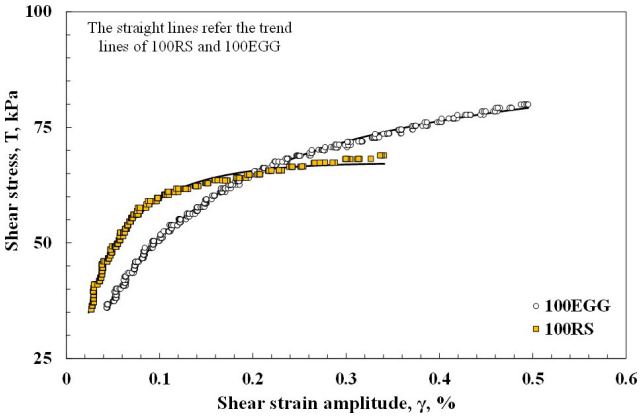

Fig. 5 Stress and strain variation of 100RS and 100EGG

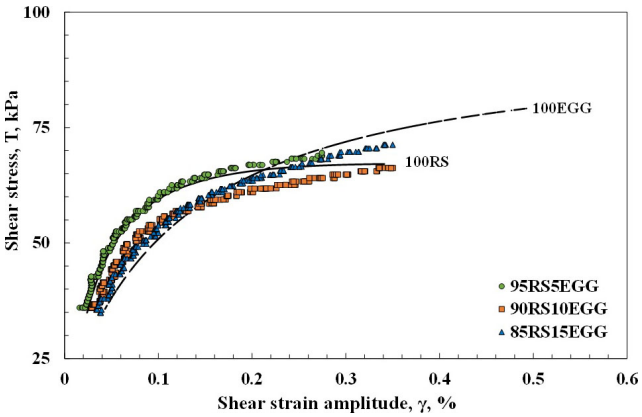

Fig. 7 Stress and strain variation of 95RS5EGG, 90RS10EGG and 85RS15EGG

4.2 Shear modulus and shear strain results

The shear modulus graphs for 100RS and 100EGG, shown in Fig. 8, indicate that the shear modulus of 100RS is considerably higher than that of 100EGG for shear strains between 0.02% and 0.1%, aligning with the stress-shear deformation amplitude relationship. The relative density of 100RS is 7.7 times greater than that of 100EGG. Conversely, 100EGG exhibits superior resistance to decreases in shear modulus compared to 100RS, due to its high internal friction angle.

Fig. 9 shows the shear modulus variation for the 99RS1EGG and 98RS2EGG specimens over a shear strain range of 0.02% to 0.4%. The shear modulus values for the 98RS2EGG specimen consistently exceed those of the 100RS over the shear strain amplitudes examined, which is attributed to effective void closure and a high angle of internal friction of EGG. A similar trend can be seen in the 99RS1EGG specimen, which shows comparable, although less pronounced, behavior at shear strain amplitudes of 0.02% to 0.07%. For shear strain amplitudes of 0.07% to 0.4% the shear modulus values for 99RS1EGG are close to those of 100RS.

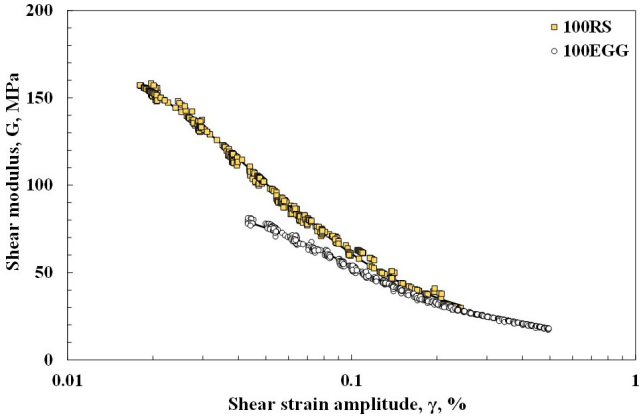

Fig. 8 Modulus and strain variation of 100RS and 100EGG

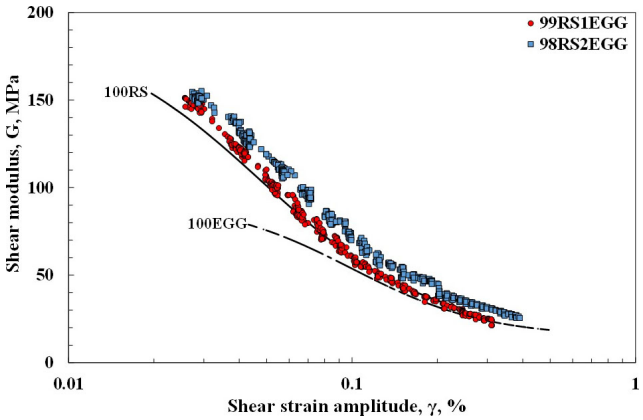

Fig. 9 Modulus and strain variation of 99RS1EGG and 98RS2EGG

Fig. 10 illustrates the shear modulus variations for the 95RS5EGG, 90RS10EGG, and 85RS15EGG specimens, spanning shear strain amplitudes of 0.02% to 0.4%. Despite being 5% lighter than 100RS, 95RS5EGG demonstrates slightly higher shear modulus values between 0.02% and 0.05% due to enhanced void filling by EGG. Its shear modulus values align with those of 100RS from 0.05% to 0.3%. In contrast, 90RS10EGG and 85RS15EGG exhibit comparable behavior with lower shear modulus values than 100RS at 0.02% to 0.1%, mainly because of their lower dry unit densities of 9% and 14% compared to 100RS. Between shear strain amplitude 0.1%–0.4%, the shear modulus values of 90RS10EGG and 85RS15EGG followed a similar trend with the shear modulus values of 100RS (Fig. 10).

4.3 Modulus reduction and accumulated energy results

Fig. 11 illustrates the relationship between modulus reduction and accumulated energy dissipation for 100RS and 100EGG. Although 100EGG is 7.7 times lighter than 100RS in specific gravity (G_S), it requires

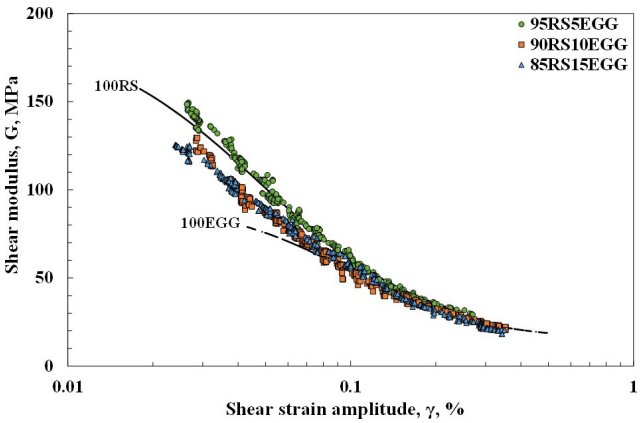

Fig. 10 Modulus and strain variation of 95RS5EGG, 90RS10EGG and 85RS15EGG

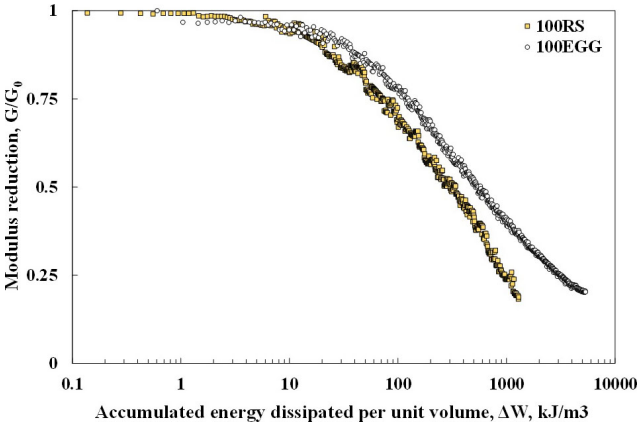

Fig. 11 Modulus reduction and accumulated energy of 100RS and 100EGG

considerably more energy to reduce its shear modulus. After G/G_0 = 0.25, the modulus reduction for 100EGG stabilizes while its accumulated energy increases, indicating that more energy is needed for 100EGG than for 100RS, highlighting EGG's high internal friction angle advantage.

Fig. 12 shows the modulus reduction versus accumulated energy dissipation for 99RS1EGG and 98RS2EGG. The 99RS1EGG specimen mirrors the trend of 100RS up to G/G_0 = 0.3, after which the influence of EGG from void filling and its high internal friction angle becomes evident. The 98RS2EGG exhibits a similar effect after G/G_0 = 0.4 and shows slightly higher modulus reduction values than 100RS. Both specimens tend to plateau in modulus reduction after these ratios, akin to 100EGG. Notably, the energy dissipation needed to reduce the shear modulus of both samples, particularly at shear strain levels exceeding 0.2%, is greater than that of 100RS.

Modulus reduction against accumulated energy dissipation graphs of mixture samples prepared by volume were shown in Fig. 13. 95RS5EGG followed a similar trend with RS100 throughout the testing process although slightly higher at low shear strain levels (0.02–0.035%). 90RS10EGG and 85RS15EGG showed lower values than RS100 up to G/G_0 = 0.4 compared to 100RS specimen, just like the shear modulus variation. After G/G_0 = 0.4, both specimens obtained higher values than RS100, until the end of the experiment. The modulus reduction values for 95RS5EGG, 90RS10EGG and 85RS15EGG show slight differences from the bulk specimens at initial shear strains (0.02–0.04%), especially up to G/G_0 = 0.75, due to void filling from test vibrations. The internal friction angle of EGG significantly affects results beyond this range. The modulus reduction curves for 90RS10EGG and 85RS15EGG flatten after G/G_0 = 0.2, a trend that is less pronounced in 95RS5EGG, which contains less EGG.

The accumulated energy values of mixed and reference samples corresponding to modulus reduction value they had during the test are given in Figs. 14 and 15 respectively.

As can be seen, the amount of energy required for the decrease in the shear modulus of the EGG additive samples

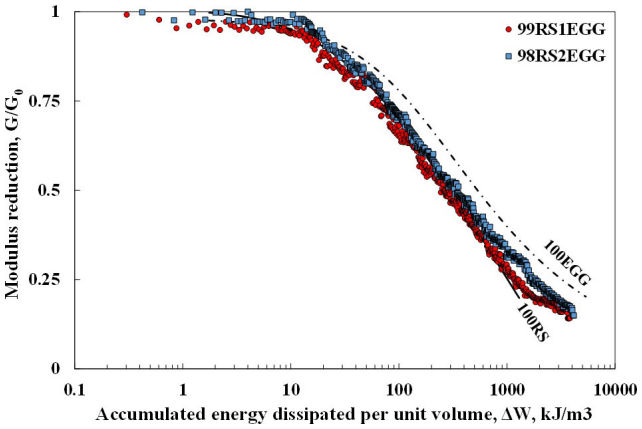

Fig. 12 Modulus reduction and accumulated energy of 99RS1EGG and 98RS2EGG

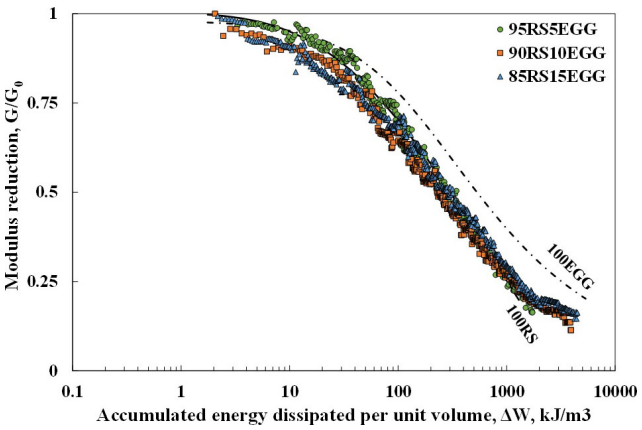

Fig. 13 Modulus reduction and accumulated energy of 95RS5EGG, 90RS10EGG and 85RS15EGG

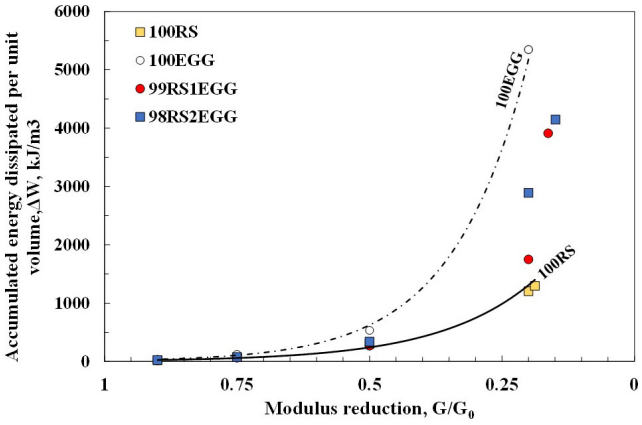

Fig. 14 Accumulated energy values of mass-prepared samples (99RS1EGG, 98RS2EGG)

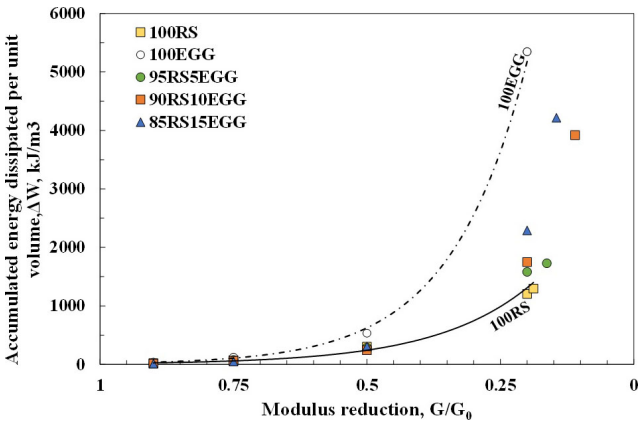

Fig. 15 Accumulated energy values of volume-prepared samples (95RS5EGG, 90RS10EGG, 85RS15EGG)

were higher compared to RS100, especially as the shear strain amplitude increased. The high internal friction angle value of EGG is thought to trigger this effect.

5 Conclusions

The principal objective of this experimental study is to examine the dynamic response of a composite material comprising RS and EGG. An energy-based approach was employed to perform dynamic torsional shear testing, with the objective of analyzing the behavior of the mixed specimens. The dry mixtures were prepared with mass proportions of 1% to 2% and volumetric proportions of 5%, 10%, and 15%. The specimens were examined under cyclic loading conditions, with a constant stress of 100 kPa. Given that EGG is inert, the observed results can be explained by the mechanical contacts between RS and EGG.

Experimental findings reveal that EGG fills the granular soil structure within the γ = 0.02–0.07% range, resulting in notable soil compaction and enhancing the shear modulus of the 99RS1EGG and 95RS5EGG mixtures. The 98RS2EGG sample exhibited higher shear modulus values at all shear strain amplitudes compared to RS100. Although the shear modulus values for the 90RS10EGG and 85RS15EGG specimens were lower than RS100 at shear deformation levels of 0.02%–0.1%, they remained approximately 20% lower at most.

The resistance of the modulus reduction of RS to reduction, evidenced by the modulus reduction graphs, can be attributed to the significantly major angle of internal friction of EGG. When the accumulated energy and modulus reduction changes are examined, the amount of energy required for the modulus value to decrease for each mixed samples are significantly higher compared to RS100, especially at increasing shear strain amplitude.

The studies conducted by Umu [24] and Yaghoubi et al. [27], which examined the interactions between clay and RG mixtures, it was evident that the shear modulus and resilient modulus of mixed samples with RG were elevated [27]. These findings were also corroborated in this study at high shear strain amplitudes.

This research paper emphasizes the usability of EGG in shallow soil improvement practices, demonstrating its considerable potential in this field. The experimental findings suggest that, based on the defined boundary conditions, their use is a viable approach. It would be beneficial to conduct further research into the efficacy of alternative soil improvement agents, such as EGG, to gain a deeper understanding of their potential for soil practices under various test constraints and soil gradations.

Acknowledgement

This study was supported by the Eskisehir Technical University Scientific Research Commission (PN:24ADP066).

References

[1] Disfani, M. M., Arulrajah, A., Bo, M. W., Hankour, R. "Recycled crushed glass in road work applications", Waste Management, 31(11), pp. 2341–2351, 2011. https://doi.org/10.1016/j.wasman.2011.07.003

[2] Tam, V. W. Y., Tam, C. M. "A review on the viable technology for construction waste recycling", Resources, Conservation and Recycling, 47(3), pp. 209–221, 2006. https://doi.org/10.1016/j.resconrec.2005.12.002

[3] Ferdous, W., Manalo, A., Siddique, R., Mendis, P., Yan, Z., Wong, H. S., Lokuge, W., Aravinthan, T., Schubel, P. "Recycling of landfill wastes (tyres, plastics and glass) in construction - A review on global waste generation, performance, application and future opportunities", Resources, Conservation and Recycling, 173, 105745, 2021. https://doi.org/10.1016/j.resconrec.2021.105745

[4] Akinade, O. O., Oyedele, L. O. "Integrating construction supply chains within a circular economy: An ANFIS-based waste analytics system (A-WAS)", Journal of Cleaner Production, 229, pp. 863–873, 2019. https://doi.org/10.1016/j.jclepro.2019.04.232

[5] Ghorbani, B., Arulrajah, A., Narsilio, G., Horpibulsuk, S., Bo, M. W. "Dynamic characterization of recycled glass-recycled concrete blends using experimental analysis and artificial neural network modeling", Soil Dynamics and Earthquake Engineering, 142, 106544, 2021. https://doi.org/10.1016/j.soildyn.2020.106544

[6] Sommariva, L., Weinberger, K. "Energy and Natural Resources Saving In The Production of Expanded Glass Granules", Chemical Engineering Transactions, 43, pp. 2437–2442, 2015. https://doi.org/10.3303/CET1543407

[7] Jaber, N. H., Radhi, M. S., Alsaad, A. J. "Sustainable Potentials of Plastics Waste-cement Kiln Dust Blends on Strength Properties of Subbase Soil", Periodica Polytechnica Civil Engineering, 67(2), pp. 596–602, 2023 https://doi.org/10.3311/PPci.21689

[8] Youssef Abd El-Latif, M., Lotfy Fayed, A., Hassan, M. "Sustainable Stabilization of Poorly Graded Desert Sand by Cement Kiln Dust and Salt Water for Using in Backfilling and Subbase Layers", Periodica Polytechnica Civil Engineering, 67(4), pp. 1234–1245, 2023. https://doi.org/10.3311/PPci.21915

[9] Ashango, A. A., Patra, N. R. "Behavior of Expansive Soil Treated with Steel Slag, Rice Husk Ash, and Lime", Journal of Materials in Civil Engineering, 28(7), 06016008, 2016. https://doi.org/10.1061/(ASCE)MT.1943-5533.0001547

[10] Sarajpoor, S., Ghalandarzadeh, A., Kavand, A. "Dynamic behavior of sand-bitumen mixtures using large-size dynamic hollow cylinder tests", Soil Dynamics and Earthquake Engineering, 147, 106801, 2021. https://doi.org/10.1016/j.soildyn.2021.106801

[11] Kumar, S., Suman, S. K. "Mathematical Modeling of a Corrugated Geogrid and Geocell Reinforced Flexible Pavement Base with Interlayer Shear Performance Analysis", Periodica Polytechnica Civil Engineering, 68(3), pp. 781–796, 2024. https://doi.org/10.3311/PPci.23169

[12] Tao, G., Yuan, J., Chen, Q., Peng, W., Yu, R., Basack, S. "Chemical stabilization of calcareous sand by polyurethane foam adhesive", Construction and Building Materials, 295, 123609, 2021. https://doi.org/10.1016/j.conbuildmat.2021.123609

[13] Abdullah, H. H., Shahin, M. A., Walske, M. L., Karrech, A. "Cyclic behaviour of clay stabilised with fly-ash based geopolymer incorporating ground granulated slag", Transportation Geotechnics, 26, 100430, 2021. https://doi.org/10.1016/j.trgeo.2020.100430

[14] Bernal-Sanchez, J., Leak, J., Barreto, D. "Rubber-soil mixtures: use of grading entropy theory to evaluate stiffness and liquefaction susceptibility", Bulletin of Earthquake Engineering, 21(8), pp. 3777–3796, 2023. https://doi.org/10.1007/s10518-023-01673-3

[15] Nikitas, G., Bhattacharya, S. "Experimental study on sand-tire chip mixture foundations acting as a soil liquefaction countermeasure", Bulletin of Earthquake Engineering, 21(8), pp. 4037–4063, 2023. https://doi.org/10.1007/s10518-023-01667-1

[16] Yin, Z., Sun, H., Jing, L., Dong, R. "Geotechnical Seismic Isolation System Based on Rubber-Sand Mixtures for Rural Residence Buildings: Shaking Table Test", Materials, 15(21), 7724, 2022. https://doi.org/10.3390/ma15217724

[17] da Silva, R. C., Puglieri, F. N., de Genaro Chiroli, D. M., Bartmeyer, G. A., Kubaski, E. T., Tebcherani, S. M. "Recycling of glass waste into foam glass boards: A comparison of cradle-to-gate life cycles of boards with different foaming agents", Science of The Total Environment, 771, 145276, 2021. https://doi.org/10.1016/j.scitotenv.2021.145276

[18] Rodrigues, C., König, J., Freire, F. "Prospective life cycle assessment of a novel building system with improved foam glass incorporating high recycled content", Sustainable Production and Consumption, 36, pp. 161–170, 2023. https://doi.org/10.1016/j.spc.2023.01.002

[19] CEN "EN 13055:2016 Lightweight aggregates", European Committee for Standardization, Brussels, Belgium, 2016.

[20] Stikloporas "Expanded glass", [online] Available at: https://stikloporas.com/expanded-glass [Accessed: 26 August 2024]

[21] Disfani, M. M., Arulrajah, A., Bo, M. W., Sivakugan, N. "Environmental risks of using recycled crushed glass in road applications", Journal of Cleaner Production, 20(1), pp. 170–179, 2012. https://doi.org/10.1016/j.jclepro.2011.07.020

[22] Kazmi, D., Serati, M., Williams, D. J., Qasim, S., Cheng, Y. P. "The potential use of crushed waste glass as a sustainable alternative to natural and manufactured sand in geotechnical applications", Journal of Cleaner Production, 284, 124762, 2021. https://doi.org/10.1016/j.jclepro.2020.124762

[23] Senanayake, M., Arulrajah, A., Maghool, F., Horpibulsuk, S. "Evaluation of rutting resistance and geotechnical properties of cement stabilized recycled glass, brick and concrete triple blends", Transportation Geotechnics, 34, 100755, 2022. https://doi.org/10.1016/j.trgeo.2022.100755

[24] Umu, S. U. "Assessment of sustainable expanded glass granules for enhancing shallow soil stabilization and dynamic behaviour of clay through resonant column tests", Engineering Science and Technology, an International Journal, 42, 101415, 2023. https://doi.org/10.1016/j.jestch.2023.101415

[25] Baldovino, J. J. A., Izzo, R. L. S., Rose, J. L., Domingos, M. D. I. "Strength, durability, and microstructure of geopolymers based on recycled-glass powder waste and dolomitic lime for soil stabilization", Construction and Building Materials, 271, 121874, 2021. https://doi.org/10.1016/j.conbuildmat.2020.121874

[26] Saberian, M., Li, J., Boroujeni, M., Law, D., Li, C.-Q. "Application of demolition wastes mixed with crushed glass and crumb rubber in pavement base/subbase", Resources, Conservation and Recycling, 156, 104722, 2020. https://doi.org/10.1016/j.resconrec.2020.104722

[27] Yaghoubi, E., Yaghoubi, M., Guerrieri, M., Sudarsanan, N. "Improving expansive clay subgrades using recycled glass: Resilient modulus characteristics and pavement performance", Construction and Building Materials, 302, 124384, 2021. https://doi.org/10.1016/j.conbuildmat.2021.124384

[28] Xiao, Y., Long, L., Evans, T. M., Zhou, H., Liu, H., Stuedlein, A. W. "Effect of Particle Shape on Stress-Dilatancy Responses of Medium-Dense Sands", Journal of Geotechnical and Geoenvironmental Engineering, 145(2), 04018105, 2019. https://doi.org/10.1061/(ASCE)GT.1943-5606.0001994

[29] Dobry, R., Ladd, R. S., Yokel, F. Y., Chung, R. M., Powell, D. "Prediction of Pore Water Pressure Buildup and Liquefaction of Sands During Earthquakes by the Cyclic Strain Method", U.S. Department of Commerce, Washington, DC, USA, 1982.

[30] Seed, H. B., Idriss, I. M. "Simplified Procedure for Evaluating Soil Liquefaction Potential", Journal of the Soil Mechanics and Foundations Division, 97(9), pp. 1249–1273, 1971. https://doi.org/10.1061/JSFEAQ.0001662

[31] Figueroa, J. L., Saada, A. S., Liang, L., Dahisaria, N. M. "Evaluation of Soil Liquefaction by Energy Principles", Journal of Geotechnical Engineering, 120(9), pp. 1554–1569, 1994. https://doi.org/10.1061/(ASCE)0733-9410(1994)120:9(1554)

[32] Jain, A., Mittal, S., Shukla, S. K. "Energy-based approach to study liquefaction triggering in homogeneous and stratified soils under consolidated undrained cyclic loading", Engineering Geology, 321, 107151, 2023. https://doi.org/10.1016/j.enggeo.2023.107151

[33] Ni, X., Ye, B., Cheng, Z., Ye, G. "Evaluation of the effects of initial deviatoric stress and cyclic stress amplitude on liquefaction potential of loose and medium-dense sands: An energy-based method", Soil Dynamics and Earthquake Engineering, 136, 106236, 2020. https://doi.org/10.1016/j.soildyn.2020.106236

[34] Berrill, J. B., Davis, R. O. "Energy Dissipation and Seismic Liquefaction of Sands: Revised Model", Soils and Foundations, 25(2), pp. 106–118, 1985.
https://doi.org/10.3208/sandf1972.25.2_106

[35] Davis, R. O., Berrill, J. B. "Pore Pressure and Dissipated Energy inEarthquakes—Field Verification", Journal of Geotechnical and Geoenvironmental Engineering, 127(3), pp. 269–274, 2001.
https://doi.org/10.1061/(ASCE)1090-0241(2001)127:3(269)

[36] Pan, K., Yang, Z. X. "Evaluation of the Liquefaction Potential of Sand under Random Loading Conditions: Equivalent Approach Versus Energy-Based Method", Journal of Earthquake Engineering, 24(1), pp. 59–83, 2020.
https://doi.org/10.1080/13632469.2017.1398693

[37] Ishihara, K. "Soil Behaviour in Earthquake Geotechnics", Clarendon Press, 1996. ISBN 9780198562245
https://doi.org/10.1093/oso/9780198562245.001.0001

[38] Okur, V., Umu, S. U. "Energy approach to unsaturated cyclic strength of sand", Bulletin of Earthquake Engineering, 11(2), pp. 503–519, 2013.
https://doi.org/10.1007/s10518-012-9396-1

[39] Okur, V., Ansal, A. "Evaluation of Cyclic Behavior of Fine-Grained Soils Using the Energy Method", Journal of Earthquake Engineering, 15(4), pp. 601–619, 2011.
https://doi.org/10.1080/13632469.2010.507298

[40] Voznesensky, E. A., Nordal, S. "Dynamic instability of clays: an energy approach", Soil Dynamics and Earthquake Engineering, 18(2), pp. 125–133, 1999.
https://doi.org/10.1016/S0267-7261(98)00043-8

[41] Drnevich, V. P. "Recent Developments in Resonant Column Testing", In: Proceedings of a session at the ASCE National Convention, Detroit, MI, USA, 1985, pp. 79–107. ISBN 0872625079